Appl. Phys. A 78, 947–954 (2004)
DOI: 10.1007/s00339-003-2413-0

Applied Physics A
Materials Science & Processing

M. SHIRAISHI[1,✉]
T. TAKENOBU[1,*]
H. KATAURA[2]
M. ATA[1]

Hydrogen adsorption and desorption in carbon nanotube systems and its mechanisms

[1] Materials Laboratories, SONY Corporation, Shin-Sakuragaoka 2-1-1, Hodogaya-ku, Yokohama 240-0036, Japan
[2] Department of Physics, Faculty of Science, Tokyo Metropolitan University, Minami-Osawa, Hachioji, Tokyo 192-0397, Japan

Received: 18 September 2003/Accepted: 30 September 2003
Published online: 9 March 2004 •

ABSTRACT The hydrogen physisorption properties in single-walled carbon nanotube (SWNT) based materials were characterized. The SWNTs were highly purified and three useful pores for hydrogen physisorption were activated. Hydrogen was physisorbed in intra-tube pores at room temperature and the capacity was estimated to be about 0.3–0.4 wt. % at room temperature. The adsorption capacity can be explained by the Langmuir model. The intra-tube pores have large adsorption potential and this induces hydrogen physisorption at comparatively higher temperatures. This fact indicates the importance of fabricating sub-nanometer ordered pores for this phenomena.

PACS 51.30.+i; 51.90.+r; 81.05.Tp; 81.07.De

1 Introduction

Since their discovery in 1991 [1], carbon nanotubes have attracted much expectation to store hydrogen because they have cylindrical structures and hollow spaces inside of their sidewalls. Novel carbonaceous materials for hydrogen storage are strongly needed for fuel cell (FC) devices because conventional hydrogen storage materials are too heavy for compact FC devices and, on the other hand, carbon is light, stable and abundant.

The pioneer work by Dillon et al. [2] on the possibility of 5–10 wt. % storage in single-walled carbon nanotubes (SWNTs) [3] at room temperature aroused interest towards SWNTs and other carbonaceous materials in this research field [4–7]. However, it was very difficult to fabricate apparatus for precise measurements because the leakage problem of high-pressure hydrogen was serious, and much attention should have been paid to the measurement of the change of introduced hydrogen pressure because, in some cases, the temperature dependence of hydrogen pressure (before equilibrium) was believed to be the evidence of hydrogen sorption. In addition, the lack of understanding about sorption prevented the obtainment of reliable results (for instance the origin of abnormally high value of sorption cannot be fully explained). Thus, further efforts were awaited for establishment of fully reproducible and convincing data [8–13]. In particular, a question remained as to whether the adsorption site for hydrogen existed in carbon at moderate temperature. At present, about 7 wt. % of hydrogen desorption from nanographite at high temperature ($\sim$ 700 K) [14] and the storage of 8 wt. % of hydrogen in SWNTs at low temperature (80 K) [15] have so far been believed to be reliable.

This report is focusing on detailed analyses of hydrogen adsorption in carbon nanotube systems and its mechanisms. Hydrogen physisorption at room temperature was characterized by using SWNTs and C_{60} encapsulated SWNTs (peapods), and the physisorption was achieved by fabricating and activating sub-nanometer scaled pores. The adsorption potential of the pores was estimated to be about -0.21 eV and this large potential induced the physisorption [16, 17]. Molecular dynamics of hydrogen adsorbed in the pores was also characterized by nuclear magnetic resonance and the result suggested the hydrogen strongly interacts with the sidewalls of the SWNTs [18]. Future prospects and a guideline of material designing are summarized in the end of the report.

2 Experiments

SWNTs were synthesized by Nd : YAG laser ablation using Ni/Co catalysts. The metal/carbon target was heated to 1200 °C in a furnace. The diameter of the SWNTs is typically 1.4 nm. For purification, carbon soot containing the SWNTs was refluxed in an aqueous solution of H_2O_2 for 3 h. After removal of any amorphous carbon, the sample was treated with HCl overnight to eliminate the remaining catalytic metals. A thermo-gravimetric analysis of this product showed that the metal contents were decreased less than 3 wt. %. For further purification, the purified SWNTs were treated with aqueous NaOH [16, 19, 20]. Small particles of by-products in the H_2O_2 purification, amorphous carbon, which covered a surface of the SWNTs and occupied inter-tube pores, were removed in this process by ultrasonication in the NaOH (pH=10–11) for 2 h. The effect of the NaOH treatment was checked by the change in Raman spectra. The intensity ratio of the G- to the D-band (G/D) changed from 50 to 90 after this treatment; this observation indicates that the amorphous carbon particles were

✉ Fax: +81-45/353-6904, E-mail: Masashi.Shiraishi@jp.sony.com
*_Current adress:_ Institute of Materials Research, Tohoku University, 2-1-1 Katahira, Aoba-ku, Sendai 980-8577, Japan and CREST, JST (Japan Science and Technology Corporation)

removed and the SWNTs were cleaned. Transmission electron microscopy (TEM) measurements also verified the cleaning of the SWNTs. Figure 1 shows that amorphous carbon particles coated the surface of the SWNTs before treatment, whereas they were removed and the sidewalls of the SWNTs were clearly seen after the treatment. It is concluded from these characterizations that the NaOH treatment is effective for cleaning the sidewalls and that the resulting SWNT-bundles have minute inter-tube pores suitable for hydrogen adsorption.

A peapod is a new form of a SWNT-based material which has unique physical properties [21–28]. The inside of peapods is filled with C_{60} molecules (or other fullerenes and metallofullerenes) and peapods differ from SWNTs only in this structural point. This structural difference is suitable to examine the gas adsorption sites in SWNT-based materials. In this work, peapods (C_{60}@SWNTs) were synthesized [23] from the same batch of the SWNTs after the NaOH treatment. The filling rate of C_{60}s in the SWNTs was estimated to be about 85% [24]. After washing the sample by toluene to remove unreacted C_{60} on the sidewalls [23], the sample was heated in a vacuum to completely eliminate the toluene. The whole procedure for sample preparation is summarized in Fig. 2.

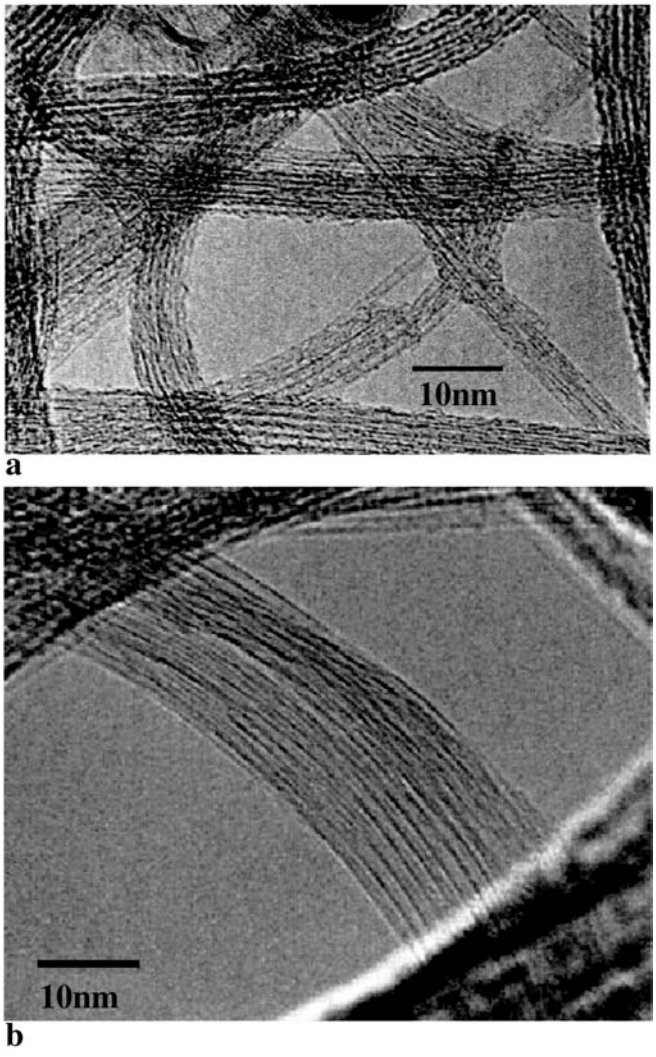

FIGURE 1 TEM photographs of purified SWNTs. **a** Before NaOH treatment, in which case many tube sidewalls were covered with amorphous carbon clusters. **b** After NaOH treatment, by which carbon clusters were removed and sidewalls were clearly seen

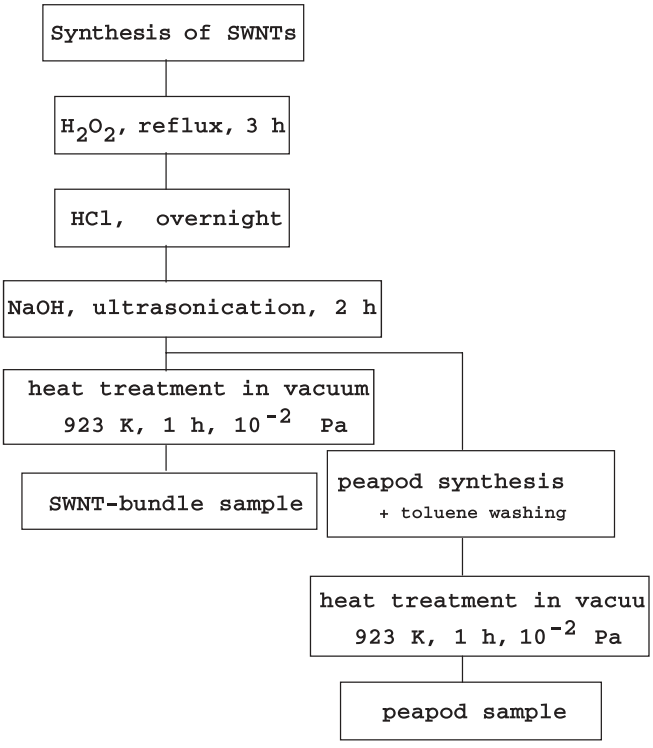

FIGURE 2 Detailed procedures for a sample preparation

Hydrogen desorption was studied by a custom-made temperature-programmed-desorption (TPD) system, by which desorption of the gaseous species was measured as a function of temperature under about 10^{-5} Pa [2]. A pretreatment condition of the samples was $T = 873$ K, $P = 10^{-4}$ Pa for 1 h. The pretreatment of the sample is a critical procedure for the adsorption and desorption of hydrogen. The purity of hydrogen was 99.99999%. The applied pressure was 6 MPa and ca. 0.1 MPa at room temperature, and the pressure dependence of the hydrogen desorption can be of help to distinguish whether hydrogen was extrinsically introduced or not.

Hydrogen adsorption capability was measured up to 9 MPa, and care was taken to eliminate the leakage of the system for precise measurements. The amount of the SWNTs was increased to about 1 g to suppress the error bar, and the volume of the applied hydrogen was evaluated with allowance for the temperature effect and by taking sufficient time to let hydrogen reach equilibrium.

A nuclear magnetic resonance (NMR) study was carried out to obtain information about the molecular dynamics of the hydrogen trapped in the inter-tube pores, as in the case of H_2 in a C_{60} solid [29]. We performed a solid-state ^{1}H magic angle spinning (MAS) NMR observation of the hydrogen at 293 K with a CMX-300 Infinity (Chemagnetics Co.; 298.99 MHz) after introducing hydrogen at 9 MPa for 5 days. The MAS was adopted at 3000 rpm because of the low intensity of the spectral pattern of the powder. The inversion recovery method was used for determination of the spin-lattice relaxation time, T_1, with the application of a $\pi/\tau/\pi/2$ pulse sequence. Therefore, the T_1 obtained under rotation is $T_{1\varrho}$.

3 Results and discussion

3.1 *Sorption mechanisms*

Before showing experimental results, we discuss mechanisms of adsorption. Physisorption and chemisorption are possible mechanisms of hydrogen adsorption. In chemisorption, hydrogen is covalently bonded with host materials and desorption temperature is too high (> 500 K) for commercial use. In physisorption, van der Waals force between hydrogen molecules and the host materials is a main force in stabilizing hydrogen on the surface. The desorption temperature is generally near room temperature, and so physisorption is much more preferable for industrial applications. Thus, we focus only on the physisorption of hydrogen in SWNTs.

Physisorption is controlled by a relation between the chemical potential of gases, μ, and adsorption potential of solids, ε. Coverage of adsorption sites, f, is determined by the Langmuir adsorption isotherm, typically

$$f = \frac{1}{1+\exp\left(\frac{\varepsilon-\mu}{kT}\right)} . \tag{1}$$

When $\varepsilon = \mu$, the coverage is equal to 0.5 and this means about 4 wt. % of hydrogen adsorption. Temperature and pressure dependence of the chemical potential of hydrogen gas, μ, shown in Fig. 3, was calculated by using the experimental values of enthalpy, H, entropy, S, taken from [30] and (2),

$$G = H - TS,$$

$$\mu = \frac{\partial G}{\partial n} , \tag{2}$$

where G is Gibbs free energy and n is a number of molecules. The adsorption potential of the inside and outside of an individual SWNT has been estimated to be at most -0.09 eV [31]. Thus, one can see that hydrogen adsorption on the outer surface and the intra-tube pores can occur only at low temperature. According to Ye et al. [15], the hydrogen adsorption amount at 80 K is about 8 wt. %, the coverage f being nearly equal to 1. This value seems to be a reasonable estimate, because the chemical potential of hydrogen is small enough at such a low temperature. To the contrary, one cannot expect hydrogen physisorption at room temperature unless the adsorption potential is significantly enhanced by modification of adsorption pore structures. In our material systems, the inter-tube pores are small enough and one can expect that they have large adsorption potential, as mentioned in the following subsections.

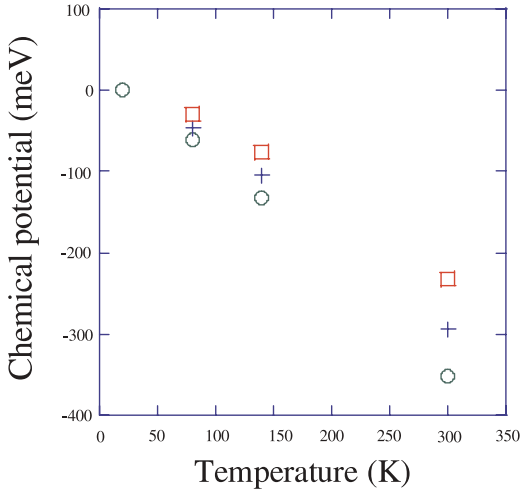

FIGURE 3 Temperature dependence of the chemical potential of hydrogen, μ. *Open circles*, *crosses* and *open squares* represent ε at 0.1, 1 and 10 MPa, respectively

3.2 *Experimental evidence for hydrogen physisorption at room temperature*

3.2.1 Results of TPD analyses. Figure 4a-d shows TPD profiles of gas desorption from the SWNTs and the peapods after application of 6 MPa and ca. 0.1 MPa of hydrogen. Hydrogen desorption was observed around 350 K from the SWNTs and the peapods which experienced only the application of high-pressure hydrogen. This fact suggests that hydrogen was introduced extrinsically and adsorbed at room temperature. Water desorption was observed only from the SWNTs, and the appearance of the peak was independent of the hydrogen pressure. These facts suggest that all sites in peapods for water adsorption were fully occupied by C_{60} molecules so that no more spaces were available.

The similarity of the hydrogen desorption profiles obtained from the SWNTs to that of the peapods suggests that the hydrogen adsorption sites in these samples are essentially the same. Because C_{60} molecules are embedded inside the tubes, the inside of the tubes cannot contribute to hydrogen adsorption. Moreover desorption temperature of about 350 K excludes the possibility of surface adsorption. Therefore, the possible sites for hydrogen adsorption are the inter-tube sites in the bundles.

Figure 5 shows size comparison of the inter- and intra-tube pores in SWNT-bundles. SWNTs form a triangular lattice, and the pore size can be estimated by taking the van der Waals radii of carbon atoms into account. Because the diameter of the SWNTs is 1.4 nm, the size of the inter-tube pores is about 0.2–0.3 nm, while the size of the intra-tube pores is about 1 nm. On the other hand, the size of water and hydrogen molecules is 0.39 and 0.24 nm, respectively. This comparison indicates that the inter-tube pores can adsorb hydrogen only when high-pressure hydrogen is applied, whereas they cannot store the water molecule because it is too large to penetrate into the inter-tube pore. Here, the size and the adsorption potential of the intra-tube pore are 1 nm and -0.09 eV, respectively. Because the size of the inter-tube pore is 0.2–0.3 nm, one can expect that the pores have larger adsorption potential which allows hydrogen physisorption. In the next subsection, we discuss a mechanism of the hydrogen adsorption.

3.2.2 Adsorption mechanisms. To determine the adsorption mechanism, a desorption energy analysis is a commonly used procedure. The relationship of the desorption energy, E_d, the heating rate, β, and the temperature at the desorption peak maximum, T_m, is represented as [32]

$$\frac{T_m^2}{\beta} = \frac{R}{E_d}\tau_0 \exp\left(\frac{E_d}{RT_m}\right) , \tag{3}$$

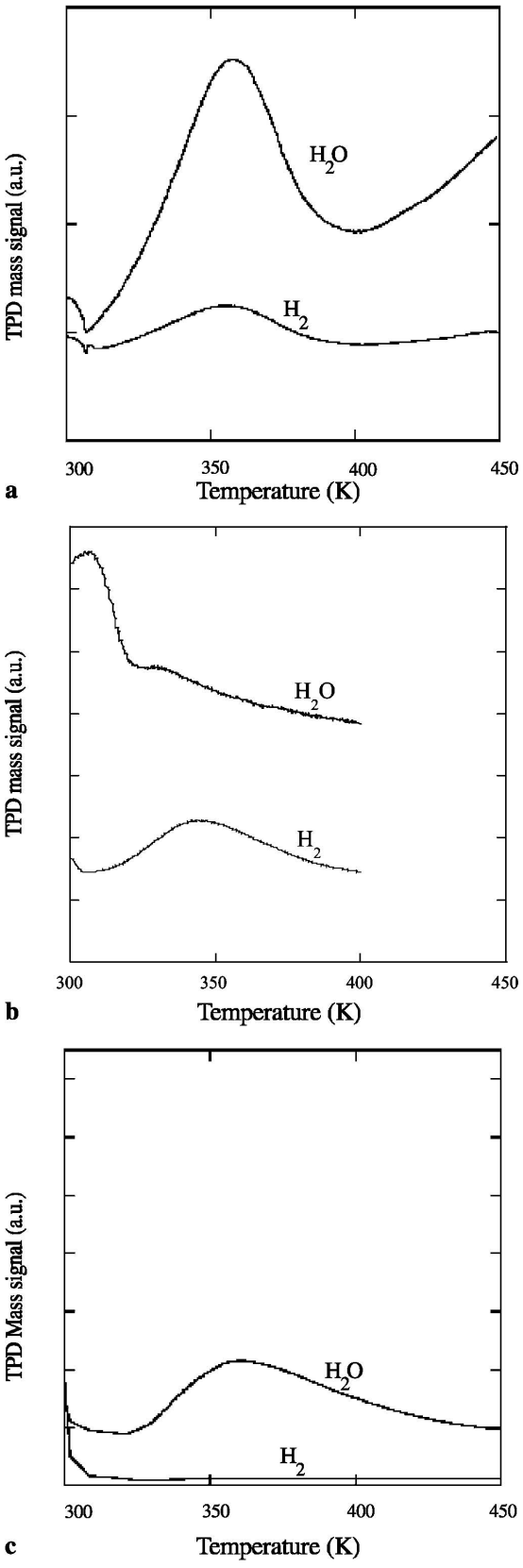

FIGURE 4 TPD observations for hydrogen and water. **a** Desorption from the SWNTs after application of 6 MPa hydrogen. Both hydrogen and water were desorbed. **b** Desorption from the peapods after application 6 MPa hydrogen. Only hydrogen was desorbed. **c** Desorption from the SWNTs after application 0.1 MPa hydrogen. **d** Desorption from the peapods after application 0.1 MPa hydrogen

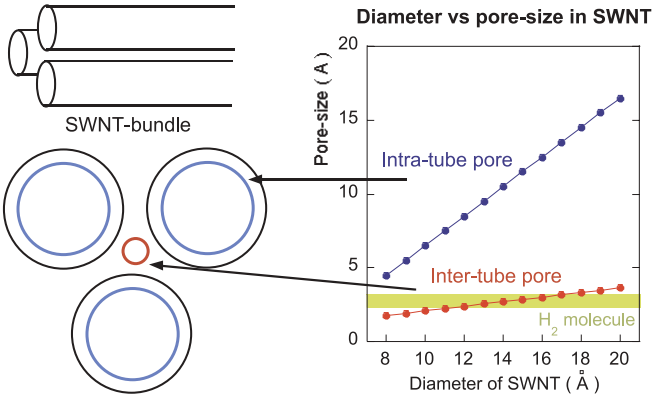

FIGURE 5 The size comparison between the intra- and the inter-tube pores and hydrogen

where R is the gas constant and τ_0 can be interpreted as the mean lifetime of the gas molecules adsorbed on a surface. The desorption energy is evaluated by changing the heating rate, as shown in Fig. 6. The estimated energy, 0.21 eV, clearly indicates that the adsorption mechanism is physisorption; if hydrogen were chemisorbed, the value should be about 10 times larger. In addition, when deuterium instead of hydrogen was introduced in the SWNTs, a similar desorption peak at 350 K was observed and the desorption energy was estimated to be about -0.20 eV. From these experimental results, we can conclude that hydrogen (and deuterium) is physisorbed at room temperature. This is the first reliable report on the hydrogen physisorption at room temperature by using well-purified SWNTs.

The estimated desorption energy can be regarded as the adsorption potential of the inter-tube pores when the surface of the pores is clean enough [32]. Equation 4 shows a relation between the desorption energy, E_d, the activation energy for adsorption, E_a, and the heat of adsorption, q,

$$E_\mathrm{d} = E_\mathrm{a} + q\,. \tag{4}$$

When the surface is clean, E_a is nearly equal to zero and q is equal to the desorption energy. In this work, the surface of the SWNTs was rinsed by NaOH and it was clean enough. Thus, the measure E_d can be regarded as the adsorption potential of the hydrogen adsorption sites, ε. As a result, the adsorption potential of the inter-tube pores is about -0.21 eV. This value is about 2.3 times larger than the calculated value of the intra-tube pores (-0.09 eV), and the minute inter-tube pores (0.2–0.3 nm) surely have larger adsorption potential. Murata et al. calculated adsorption potential of pores in nitrogen/single-walled carbon nanohorns (SWNHs) system [33]. Although the size of SWNH is 2 nm and the interaction between N_2 and SWNHs was focused, the ratio between the adsorption potential of the inter- and intra-nanohorn is 1.8, and this has good accordance with our experimental result.

3.2.3 Hydrogen adsorption capability and validity of our model. Figure 7 shows the hydrogen adsorption capability of the SWNTs. The amount of adsorbed hydrogen depends on the applied hydrogen pressure, and the storage of hydrogen at

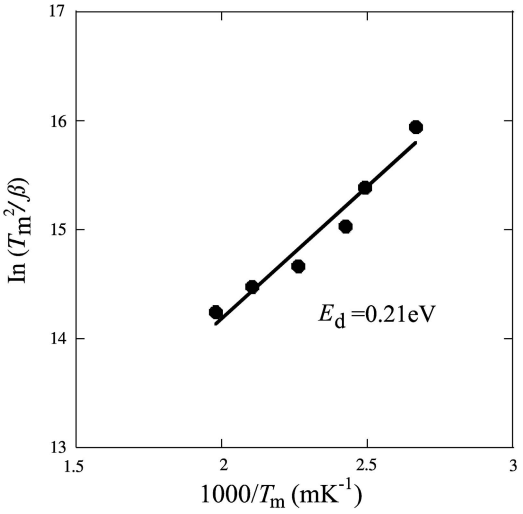

FIGURE 6 Kissinger's plot of $\ln(T_m^2/\beta)$ against $1/T_m$ with β varying from 0.017 to 0.17 K/s

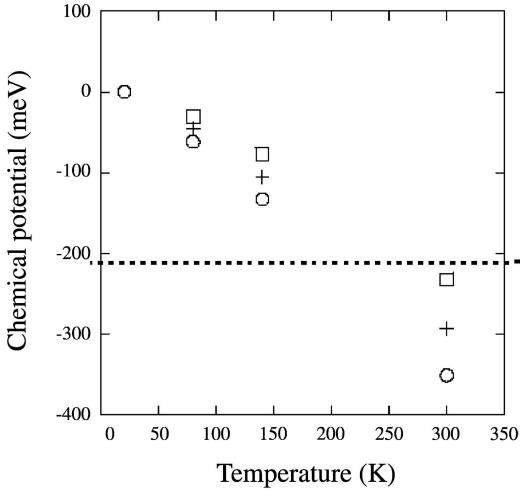

FIGURE 8 Comparison of the adsorption potential of the inter-tube pores and the chemical potential of hydrogen

9 MPa is about 0.3 wt. %. In this experimental scheme, hydrogen is adsorbed only in the inter-tube pores. The maximum amount of the adsorbed hydrogen in the inter-tube pores is limited and estimated to be about 0.8 wt. % [34]. This means that the coverage of the pore is about 0.38 in our experiments. Figure 9 shows the comparison of the adsorption potential of the inter-tube pores and the chemical potential of hydrogen. The coverage of the inter-tube pores at 300 K and 10 MPa, $f = 0.31$, as estimated from the μ value in Fig. 8 and the experimental ε value, is comparable with the measured value, 0.38. This similarity corroborates our experimental results and the Langmuir model used in this study. The corresponding coverage for the intra-tube pores, $f = 0.0044$, is smaller by two orders of magnitude, though the adsorption potential of the inter-tube pores is at most 2-3 times as large as that of the intra-tube pores. In other words, only a small difference in ε induces a major difference in f. Therefore, fabrication of minute pores, with 0.2–0.3 nm of size and with large ε, is indeed a crucial factor to achieve hydrogen physisorption at room temperature. This indicates importance of fabricating "sub-nanometer ordered" spaces.

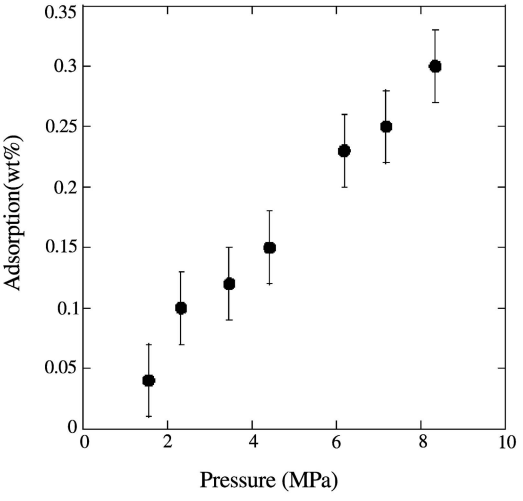

FIGURE 7 Amount of adsorbed hydrogen (wt. %) against applied hydrogen pressure, P. The error bar is estimated to be 0.03% from the precision of the pressure gauge

3.2.4 A NMR study on hydrogen trapped in SWNT-bundles. In the previous subsections, physisorption of hydrogen in SWNTs was analyzed in detail. The next concern is the condition under which hydrogen exists in the pores. In this subsection, a NMR characterization of the adsorbed hydrogen in the inter-tube pores is discussed. A NMR study can give information about the molecular dynamics of hydrogen trapped in hollow spaces, for instance, an interstitial site in solid C_{60} [29].

Figure 9a and b show the ^{1}H MAS NMR spectra observed for the no-H_2 adsorbed sample (sample A) and the H_2-adsorbed sample (sample B). A clear peak at 5.1 ppm was observed in sample B, although no peak was visible in sample A. It is notable that the peak position is close to that for water molecules [35]. Actually, liquid water has a peak at 4.96 ppm at 296.3 K. To confirm whether the peak is attributable to hydrogen or water, sample B was exposed to SO_2 gas mixed with the same volume of dry N_2 gas for 3.5 h. If the peak attributes to the remaining water molecules in the sample, the water would easily interact with the SO_2 gas and the peak would change or it would disappear. After 3.5 h exposure, no change in the peak position or the peak shape was observed (Fig. 9c). From this result and the fact that no peak was observed in sample A, it is concluded that the peak at 5.1 ppm is attributable to hydrogen molecules in the inter-tube pores. The value, 5.1 ppm, is comparable with the previously reported value of hydrogen molecules loaded in silica, 4.8 ± 0.2 ppm [36, 37]. In that work, hydrogen was loaded in the non heat-treated silica at 1.09 MPa for 70 days. As discussed later, the relaxation time T_1 in both cases is also very similar. The similarity also supports the validity of our experimental results.

Hydrogen is trapped in the inter-tube pores, as mentioned above. Judging from the size of the pores, hydrogen is trapped in the minute pores and it can interact strongly with the sidewalls of the SWNTs. The spin-lattice relaxation time, T_1, can be a good index of the strength of interaction in this case.

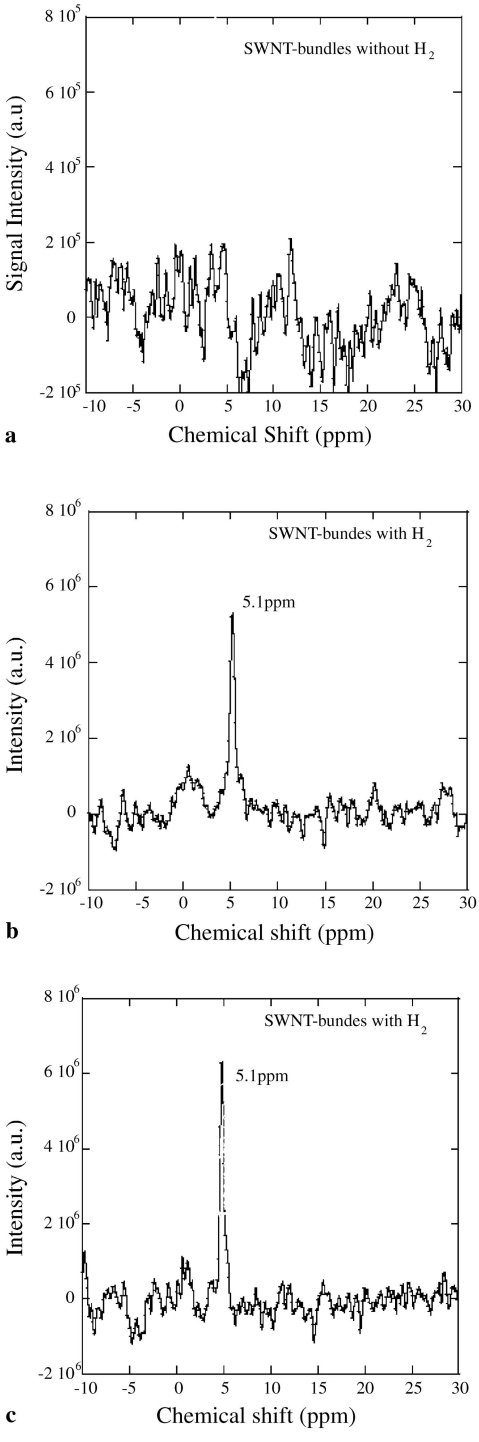

FIGURE 9 NMR signals of hydrogen in SWNTs bundles. **a** Sample A (non-adsorbed). **b** Sample B (adsorbed). **c** NMR signal from the sample B after exposure to a SO_2 and N_2 mixture for 3.5 h

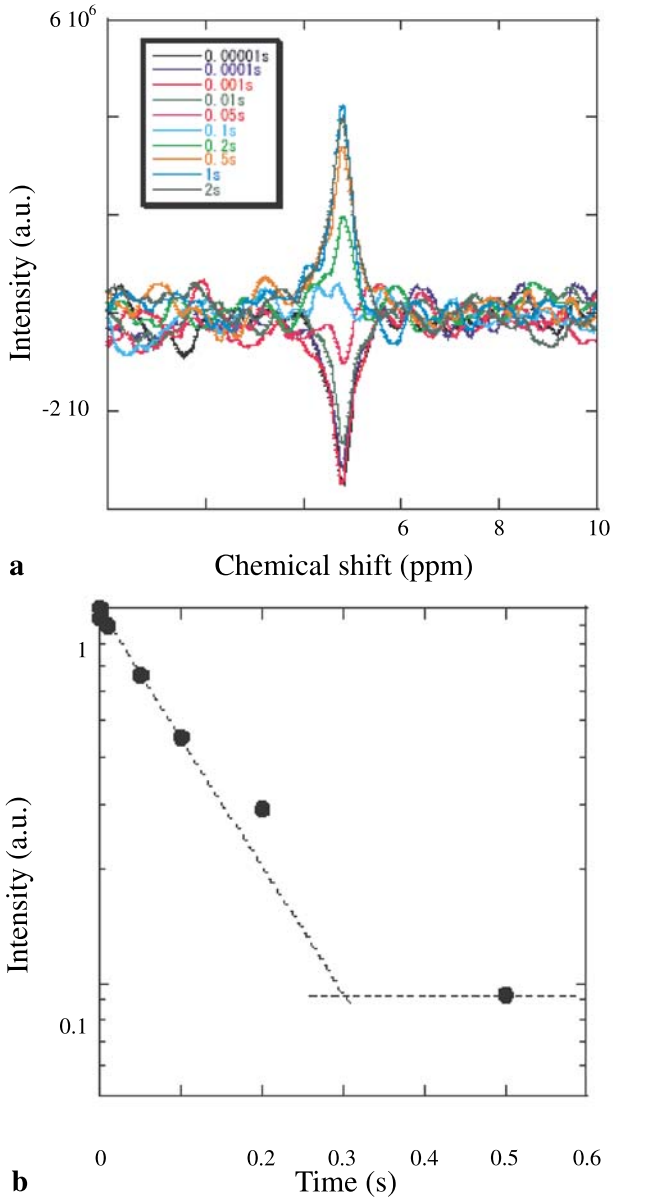

FIGURE 10 **a** The inverse recovery of the NMR signals in sample B. **b** The time dependence of the normalized peak intensity

Figure 10a shows the inverse recovery of the NMR signals, and the time dependence of the normalized peak intensity is shown in Fig. 10b. In Fig. 10b, the difference between the initial and the final intensity is regarded to be M_0, and the difference between the initial and the time-dependent intensity at each measuring time is normalized by M_0. From this result, T_1 is estimated to be about 0.1–0.2 s. T_1 of hydrogen molecules in a-Si and in silica is about 0.45 s [38] and 1 s [36], respectively. In both cases, the hydrogen molecules exist in the minute space, for instance, interstitial sites. In our case also, hydrogen is trapped tightly in the minute spaces. Therefore, the similarity of T_1 in each case can be explained by the similarity of circumstances where the hydrogen molecules exist.

4 Conclusion

In this report, the adsorption of hydrogen in SWNTs and its mechanisms were studied, and the first hydrogen physisorption at room temperature in the well-purified SWNTs and peapods was achieved by using NaOH-rinsed SWNTs. Hydrogen was adsorbed in the inter-tube pores of the SWNT-bundles, because the pores are 0.2–0.3 nm in size and, therefore, they have sufficiently large adsorption potential (-0.21 eV) for the achievement of physisorption. This suggests the importance of sub-nanometer ordered spaces. By

the ^{1}H MAS NMR measurements, it was clarified that the adsorbed hydrogen strongly interacts with the sidewalls of the SWNTs as the hydrogen does in silica and a-Si. Until this work, the research topic of hydrogen storage in SWNTs was not conclusive, but we believe that this work can be of help to understand the fundamental mechanisms.

The most important point of hydrogen physisorption in SWNT systems is to fabricate and activate minute pores. At present, the intra-tube cannot be available because they are too large for hydrogen. However, if one can succeed in synthesizing small-sized-materials encapsulated SWNTs, the intra-tube pores also become suitable spaces. Similarly, double-walled carbon nanotubes (DWNTs), SWNTs with very small diameter seem to be promising candidates. "Nanotechnology" is becoming a key term of science now, but we would like to emphasize that "Sub-nanotechnology" is also important in this field.

ACKNOWLEDGEMENTS The authors (M. S, M. A) thank Mr.Y. Murakami for his TEM observation and Dr.H. Kajiura for providing Fig. 1.

REFERENCES

1 S. Iijima: Nature **354**, 56 (1991)
2 A.C. Dillon, K.M. Jones, T.A. Bekkedahl, C.H. Kiang, D.S. Bethune, M.J. Heben: Nature **386**, 377 (1997)
3 S. Iijima, T. Ichihashi: Nature **363**, 603 (1993)
4 A.C. Dillon, T. Gennet, J.L. Alleman, K.M. Jones, P.A. Parilla, M.J. Heben: Proceedings of the 2000 Hydrogen Program Review, May 8-10, 2000; NREL/CP-570-28890, 2000
5 P. Chen, X. Wu, J. Lin, K.L. Tan: Science **285**, 91 (1999)
6 A. Chambers, C. Park, R. Terry, K. Baker, N.M. Rodriguez: J. Phys. Chem. B **102**, L4253 (1998)
7 C. Liu, Y.Y. Fan,M. Liu, H.T. Cong, H.M. Cheng, M.S. Dresselhaus: Science **286**, 1127 (1999)
8 M. Hirscher, M. Becher, M. Haluska, U. Detlaff-Weklikowska, A. Quintel, G.S. Duesberg, Y.M. Choi, P. Downes, M. Hulman, S. Roth, I. Stepanek, P. Bernier: Appl. Phys. A **72**, 129 (2001)
9 C.C. Ahn, Y. Ye, B.V. Ratnakumar, C. Witham, R.C. Bowman, B. Fultz: Appl. Phys. Lett. **72** 3378 (1998)
10 R.T. Tang: Carbon **38**, 623 (2000)
11 C. Zandonella: Nature **410**, 734 (2001)
12 G.G. Tibbetts, G.P. Meisner, C.H. Olk: Carbon **39**, 2291 (2001)
13 H. Cheng, G.P. Pez, A.C. Cooper: J. Am. Chem. Soc. **123**, 5845 (2001)
14 S. Orimo, T. Matsunaga, H. Fujii, T. Fukunaga, G. Majer: Appl. Phys. Lett. **90**, 1545 (2001)
15 Y. Ye, C.C. Ahn, C. Witham, B. Fultz, J. Liu, A.G. Rinzler, D. Colbert, K.A. Smith, R.E. Smalley: Appl. Phys. Lett. **74**, 2307 (1999)
16 M. Shiraishi, T. Takenobu, A. Yamada, M. Ata, H. Kataura: Chem. Phys. Lett. **358**, 213 (2002)
17 M. Shiraishi, T. Takenobu, M. Ata: Chem. Phys. Lett. **367**, 633 (2003)
18 M. Shiraishi, M. Ata: J. Nanosci. & Nanotech. **2**, 463 (2002)
19 A.G. Rinzler, J. Liu, H. Dai, P. Nikolaev, C.B. Hufmann, F.J. Rodriguez-Macias, P.J. Boul, A.H. Lu, D. Heymann, D.T. Colbert, R.S. Lee, J.E. Fischer, A.M. Rao, P.C. Eklund, R.E. Smalley: Appl. Phys. A **67**, 29 (1998)
20 L. Vaccarini, C. Goze, R. Aznar, V. Micholet, C. Journet, P. Bernier: Synth. Met. **103**, 2492 (1999)
21 B.W. Smith, M. Monthioux, D.E. Luzzi: Nature **296**, 323 (1998)
22 H. Kataura, Y. Maniwa, T. Kodama, K. Kikuchi, K. Hirahara, K. Suenaga, S. Iijima, S. Suzuki, Y. Achiba, W. Kraeschmer: Synth. Met. **121**, 1195 (2001)
23 H. Kataura, Y. Maniwa, M. Abe, A. Fujiwara, T. Kodama, K. Kikuchi, H. Imahori, Y. Misaki, S. Suzuki, Y. Achiba: Appl. Phys. A **74**, 349 (2002)
24 K. Hirahara, K. Suenaga, S. Bandow, H. Kato, T. Okazaki, H. Shinohara, S. Iijima: Phys. Rev. Lett. **85**, 5384 (2000)
25 S. Okada, S. Saito, A. Ishiyama: Phys. Rev. Lett. **86**, 3835 (2001)
26 T. Pichler, H. Kuzmany, H. Kataura, Y. Achiba: Phys. Rev. Lett. **87**, 267 401 (2001)
27 P.W. Chiu, G. Gu., G.T. Kim, G. Philipp, S. Roth, S.F. Yang, S. Yang: Appl Phys. Lett. **79**, 3845 (2001)
28 J. Lee, H. Kim, S.-J. Kahng, G. Kim. Y.-W. Son, J. Ihm, H. Kato, Z.W. Wang, T. Okazaki, H. Shinohara.and Y. Kuk: Nature **415**, 1005 (2002)
29 M. Tomaselli, B.H. Meier: J. Chem. Phys. **115**, 11 017 (2001)
30 R.D. McCarty, J. Hord, H.M. Roder: *Selected Properties of Hydrogen* (U.S. Depertment of Commerce, Malcolm Baldrige; U.S. Government Printing Office: Washington, DC, 1981)
31 G. Stan, M.W. Cole: J. Low Temp. Phys. **110**, 539 (1998)
32 R.J. Madix: The application of flash desorption spectroscopy to chemical reactions on surfaces: temperature programmed reaction spectroscopy. *Chemistry and Physics of Solid Surface* (CRC: Boca Raton, 63 1979)
33 K. Murata, K. Kaneko, W.A. Steele, F. Kokai, K. Takahashi, D. Kasuya, K. Hirahara, M. Yudasaka, S. Iijima: J. Phys. Chem. B **105**, 10 210 (2001)
34 A. Fujiwara, K. Ishii, H. Suematsu, H. Kataura, Y. Maniwa, S. Suzuki, Y. Achiba: Chem. Phys. Lett. **336**, 205 (2001)
35 T.J. Bastow, R.M. Hodge, A.J. Hill: J. Membr. Sci. **131**, 207 (1997)
36 Q. Zeng, J.F. Stebbins, A.D. Heaney, T. Erdogan: J. Non-cryst. Solids **258**, 78 (1999)
37 C.M. Hartwig, I. Vitko Jr.: Phys. Rev. B **18**, 3006 (1978)
38 J. Baugh, D. Han, A. Kleinhammes, C. Liu, Y. Wu, Q. Wang: J. Non-cryst. Solids **266**, 185 (2000)